Applied Physics Letters PERSPECTIVE scitation.org/journal/apl

Perspective on the band structure engineering and doping control of transparent conducting materials

Cite as: Appl. Phys. Lett. **119**, 070502 (2021); doi: 10.1063/5.0058450
Submitted: 30 May 2021 · Accepted: 24 July 2021 ·
Published Online: 18 August 2021

View Online Export Citation CrossMark

Xuefen Cai[1,2] and Su-Huai Wei[1,a)]

AFFILIATIONS

[1]Beijing Advanced Innovation Center for Materials Genome Engineering, Beijing Computational Science Research Center, Beijing 100193, China
[2]State Key Laboratory of Superlattices and Microstructures, Institute of Semiconductors, Chinese Academy of Sciences, Beijing 100083, China

[a)]Author to whom correspondence should be addressed: suhuaiwei@csrc.ac.cn

ABSTRACT

Transparent conducting materials (TCMs), which combine high electrical conductivity and high optical transmission in the visible spectral range, are needed in many modern optoelectronic devices such as solar cells, flat-panel displays, touch-screen sensors, light emitting diodes, and transparent thin film transistors. However, many physical properties of the TCMs are still not very well understood. Understanding the band structure and physical origin of the unique properties of the TCMs is, therefore, crucial for the future design of these fascinating materials. In this Perspective, we will first present a brief review of the unique band structure and doping control of TCMs. In particular, we will discuss (i) the fundamental band structures and defect properties for the TCMs and why most of them are oxides (transparent conducting oxides, TCOs); (ii) how to achieve simultaneously high transparency and conductivity in *n*-type TCMs; (iii) why *p*-type TCOs are difficult to achieve; (iv) how to modify the band structure or design new materials to achieve *p*-type TCMs or even bipolarly dopable TCMs. Finally, we will discuss some of the remaining challenges and opportunities for the development of TCMs in the near future.

Being a class of materials possessing both high electrical conductivity and high visible light transparency, transparent conducting materials (TCMs) have been extensively studied and explored in multiple applications including light emitting diodes (LEDs), solar cells, smart window, display panel, and flexible transparent devices.[1–5] The vast majority of practically used TCMs are the wide bandgap post-transition metal oxides, termed as transparent conducting oxides (TCOs). The valence band maximum (VBM) states of the prototypical TCOs, such as In_2O_3, SnO_2, and ZnO, are dominated by the low-lying and localized O 2*p* states, while the conduction band minimum (CBM) states are constructed from the antibonding state of cation *s* and oxygen *s*.[4,6,7] As such, based on the doping limit rule,[8] the *n*-type doping capability of these TCOs considerably surpasses its *p*-type doping capability. The absence of readily accessible *p*-type TCOs poses major limitations in the fabrication flexibility of transparent optoelectronic devices with essential *p*-*n* junctions such as solar cells, transparent field-effect transistors, LEDs, and semiconductor lasers.

Over the years, a large amount of experimental and theoretical research has been carried out to seek and design potential *p*-type TCOs, which has yielded notable results. In this Perspective, we will focus on some specific progresses and highlight the *key design concept* of the promising *p*-type TCMs, including the Cu^+ based ternary oxides with layered delafossite and tetragonal structures (such as $CuInO_2$ and $SrCu_2O_2$),[9–13] bismuth-alloyed β-Ga_2O_3 with the high-lying VBM state,[14] and metal halide perovskites (such as $CsPbCl_3$, $RbPbCl_3$) with an inverted band structure.[15,16] In addition to the issue of *p*-type TCMs, many fundamental physical properties of the TCMs still remain not very well understood, although significant advances have occurred in recent years. Here, we will discuss and illustrate the electronic structures, optical properties, and the physical origin of the TCMs, in combination with our theoretical work in the past two decades. More specifically, we attempt to answer the following questions in this paper: (i) What are the fundamental band structures and electrical, optical, and defect properties for the conventional TCMs? (ii) How to simultaneously raise the optical transparency and conductivity in

n-type TCMs and what are the guidelines for being a good *n*-type TCM? (iii) Why *p*-type TCMs are difficult to achieve and how to modify the crystal and electronic structures and design promising *p*-type or even bipolarly dopable TCMs? At last, some ideas and research directions for future research and design of fascinating TCMs will also be discussed.

The essential property of transparency of TCOs generally demands a wide optical bandgap larger than 3 eV. Determining the bandgaps of TCO materials, however, has not been a facile work. The process of bandgap ascertainment for the prototype *n*-type TCO, In_2O_3, is a distinct case.[17] Early experiments observed that In_2O_3 has two optical absorption onsets at ∼3.7 eV and ∼2.9 eV.[18] It was speculated that these two different onsets are caused by the indirect transition in In_2O_3, which, yet need to be confirmed by the band structure calculations on In_2O_3.[19,20] This puzzle was not resolved until 2008 when Walsh *et al.* argued that In_2O_3 has a "forbidden" small fundamental bandgap of 2.9 eV and a much larger optical bandgap of 3.7 eV by applying first-principles calculations and x-ray spectroscopy.[17] Figure 1(a) plots the schematic band levels of bixbyite In_2O_3 at the Brillouin zone center. The VBM and CBM states of In_2O_3 are both of even parity due to the inversion symmetry of its crystal structure and atomic orbital characters of the wavefunctions, which, therefore, forbids the dipole optical transition between them. A strong optical transition commences from the Γ_8^- valence state, which lies 0.81 eV below the VBM and has mostly O 2*p* character, to the Γ_1^+ CBM state, while the optical transition between other valence band states between the Γ_8^- state and the Γ_4^+ VBM state, which can be considered as folded bands due to the large bixbyite unit cell, to the CBM is extremely weak. As such, the optical bandgap of In_2O_3 is much larger than its direct fundamental bandgap by about 0.8 eV.

As another widely used TCO, the bandgap determination of SnO_2 is also a challenging task.[21] Considering the presence of inversion symmetry and the resultant forbidden VBM-CBM transition in rutile SnO_2, it is expected that, analogous to In_2O_3, SnO_2 possesses two different optical absorption onsets as well. Nonetheless, to date, there is only an experimental absorption peak at ∼3.6 eV for SnO_2 been reported,[22–24] which was argued to be originated from the allowed weak transitions from the vicinity of the VBM under intense illumination experimentally.[25,26] This argument seems plausible, but it is still unable to answer the following two questions regarding the optical and electrical measurements on SnO_2. First, why up to now, no other optical bandgap of SnO_2 has been detected and reported under low intense illumination? Second, what induces the large valence band offset between rutile SnO_2 and rutile TiO_2? Experimental measurements show that SnO_2 has a lower CBM than that of TiO_2 with a conduction band offset of ∼0.4 eV.[27,28] Taking the bandgap of rutile SnO_2 and rutile TiO_2 (3.0 eV),[29] the derived valence band offset would be as large as 1.0 eV if SnO_2 had a bandgap of 3.6 eV, contradicting to the common anion rule and *p-d* coupling models.[30,31]

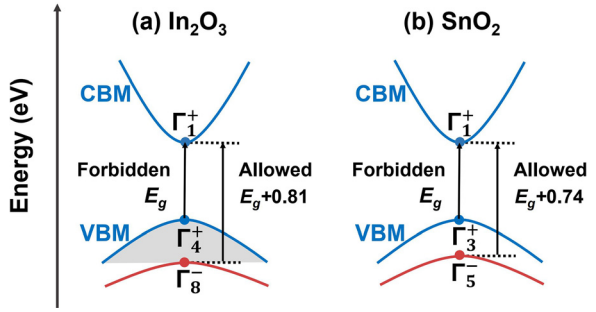

FIG. 1. Schematic diagram of band structure and energy levels of (a) bixbyite In_2O_3 and (b) rutile SnO_2 near the Γ-point. The irreducible representations of band states are shown. The superscript + (–) in the irreducible representation denotes the even- (odd-) parity band state for a semiconductor with inversion symmetry. The light gray region under the VBM of In_2O_3 indicates that there are some bands lie in the range between Γ_4^+ and Γ_8^- states due to the large bixbyite unit cell.

In a recent work, we have addressed this issue by performing first-principles calculations.[21] With HSE06 functional, the fundamental bandgap of SnO_2 is 2.96 eV, much smaller than the widely quoted value of ∼3.6 eV, while the calculated SnO_2/TiO_2 valence and conduction band offset are 0.38 eV (consistent with the common anion rule) and 0.45 eV (in line with the experimental data), respectively. Moreover, as shown in Fig. 1(b), the VBM-CBM optical transition is forbidden due to their same parities; the optical transition from the Γ_5^- valence band, 0.74 eV below the VBM, to the Γ_1^+ CBM is allowed and found to be strong. Interestingly, the calculated $\Gamma_5^- - \Gamma_1^+$ optical gap is 3.7 eV, consistent with the experimentally detected absorption onset (∼3.6 eV) of SnO_2.[22–24] Additionally, we have carefully analyzed and compared the calculated bandgap of SnO_2, TiO_2, and other metal oxides with the analogous characters of band edges by using different-level computational methods and functionals within the density functional theory. The results indicate that rutile SnO_2 should have a fundamental bandgap $(\Gamma_3^+ - \Gamma_1^+)$ of ∼3.0 eV and an optical gap $(\Gamma_5^- - \Gamma_1^+)$ of ∼3.7 eV.

Furthermore, it should be noted that for *n*-type TCOs with high concentration of electrons, the intra-band transitions among the conduction bands may reduce the optical transparency and need to be considered when estimating the performance of *n*-TCOs. For both In_2O_3 and SnO_2, the energy separation between the first (CBM) and second conduction bands reaches up to 5.0 eV[17,21] due to the high ionicity of the crystal, which explains why they are good *n*-type TCOs.

Our understanding of the electronic and optical properties for these prototype n-type TCO materials, thus, provides the following *criteria* for being a good *n*-type TCO, which can be summarized as follows:

(i) Small fundamental bandgap originated from the low CBM energy leads to the accessibility of *n*-type doping and good electrical conductivities according to the doping limit rule.[8] Specifically, to achieve such a goal, the oxides should contain large cations with a closed-shell electronic ns^0 configuration, such as In^{3+} and Sn^{4+}, so the antibonding CBM state can have low energy. Note that, these cations are also multivalent, that is, they are easy to take electrons and convert to In^{1+} and Sn^{2+} ions, and their ns^0 or ns^2 configuration indicates they have good transport properties.

(ii) Sufficiently large optical bandgap caused by dipole-forbidden transitions between band edges or indirect band gaps results in the good optical transparency. Generally, this requirement could be fulfilled using a crystal structure with inversion symmetry and a large *p-d* coupling effect.

(iii) Large separation between the first (CBM) and second conduction bands results in negligible intra-band absorptions and further guarantees transparency. This criterion hints that materials with large ionicity such as oxides are preferred.

Traditionally, it was believed that the electrons in *n*-type TCOs are provided by oxygen vacancy in these materials. However, recent theoretical calculations[7] suggest that oxygen vacancies in most of the TCOs are deep level states and, thus, cannot provide sufficient electrons to the *n*-type TCOs. Indeed, the commercially available *n*-type TCOs include Sn-doped In_2O_3 (ITO), F-doped SnO_2 (FTO), and Al-doped ZnO (AZO) all requires extrinsic doping to achieve high carrier density. Aside from the selection of appropriate extrinsic dopants, it is also crucial to understand why some of the TCOs are better to be doped on the cation site and some are on the anion site for optimal *n*-type doping. It is traditionally believed that the antibonding CBM states of semiconductors are dominated by the cation *s* orbitals (i.e., localized at the cation site); therefore, doping on the anion site may be better since it is expected to less perturb the CBMs and lead to shallow levels.[32–35] In Ref. 36, it is observed that the anion site doping (F_O) is better than the cation one (Sb_{Sn}) for SnO_2, but the cation site doping (Al_{Zn}) seems to be better than the anion site one (F_O) for ZnO. That is, the conventional wisdom works for SnO_2, but not ZnO. Using first-principles calculations and analysis, we demonstrated that this site preference is attributed to the more covalent and ionic nature of SnO_2 and ZnO. Specifically, for compounds with high ionicity, such as ZnO, its CBM state will contain large amount of unoccupied O 3*s* orbitals, i.e., its CBM charge is more localized on the O site, therefore, doping on the O site will result in large CBM perturbation and deep donor levels. In this case, it is preferable to dope on the cation site. Chemical potential analysis also suggests that for this system, doping under the O-poor condition can actually lead to high donor concentration whether the doping is on the anion site or the cation site,[8] this could be the origin why people initially believe oxygen vacancies were the dopant in oxides such as ZnO.

As stated above, the reason that oxides are difficult to be doped *p*-type is because their VBMs consist mostly O 2*p* character, so they are too low in energy. Therefore, based on the doping limit rule,[8] *p*-type doping in conventional TCO can be achieved only by increasing its VBM energy. In the following, we will discuss several approaches that the *p*-type TCM can be obtained.

The cuprous oxide, Cu_2O,[37] is an excellent *p*-type metal oxide mainly because of its shallower Cu $3d^{10}$ level compared with the O $2p^6$ level. As depicted in Fig. 2(d), the Cu 3*d* hybridizes with the O 2*p* orbital, forming the high antibonding VBM state in Cu_2O. While in other conventional oxide with $3d^{10}$ orbital such as ZnO, the Zn $3d^{10}$ orbital is deeper than the O $2p^6$ orbital, which leads to a lower antibonding *p*-*d* VBM in ZnO compared to Cu_2O. As such, the higher VBM state in Cu_2O results in a better *p*-type dopability than that of ZnO according to the doping limit rule.[8] Although the relatively small bandgap of ∼2.1 eV for Cu_2O undoubtedly restrains it as a *p*-TCO, it points out that the *p*-type TCO could probably be realized if one can appropriately modify the crystal structure of Cu_2O to enlarge its bandgap and maintaining its excellent p-type doping properties. A series of previous works have proposed that $CuAlO_2$, $SrCu_2O_2$, and their related Cu^+ based ternary oxides are the promising *p*-type TCOs.[9–13]

As shown in Fig. 2(a), Cu_2O adopts the cubic structure with the space group of $Pn\bar{3}m$.[37] It consists of a body centered cubic cell of O atoms and a face centered cubic cell of Cu atoms. The O atom is centered on the Cu_4O tetrahedra surrounded by four Cu atoms, while the Cu atom binds with two O atoms and forms the O-Cu-O dumbbell.

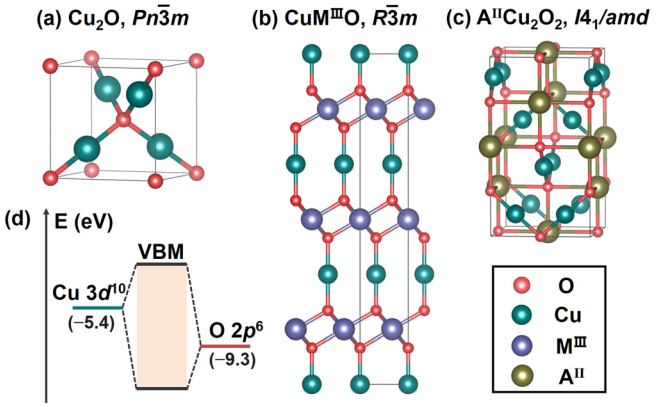

FIG. 2. The crystal structures of (a) cubic cuprite cuprous oxide (Cu_2O), (b) rhombohedral delafossite $CuM^{III}O_2$ (M^{III}=Al, Ga, In), and (c) tetragonal $A^{II}Cu_2O_2$ (A^{II}=Mg, Ca, Sr, Ba). (d) The schematic diagram of orbital interaction between Cu 3*d* and O 2*p*. The atomic orbital energies of Cu 3*d* and O 2*p* are given in parentheses. The antibonding *p*-*d* state forms the VBM of Cu_2O.

The Cu atoms form an fcc sublattice and each has 12 nearest-neighbor Cu atoms, and the Cu-Cu distance is small. The strong *d*-*d* coupling between the Cu atoms is a main reason for the small bandgap of Cu_2O besides the high *d* level and O *p*-Cu *d* coupling,[13,38,39] thus, to increase the bandgap, one should reduce the Cu *d*-*d* coupling.

The crystal structure of delafossite $CuM^{III}O_2$,[9,12] where M^{III}=Al, Ga, and In, is able to weaken the strength of Cu *d*-*d* coupling by inserting a metal layer between the O-Cu-O dumbbell layers. As shown in Fig. 2(b), $CuM^{III}O_2$ has a layered rhombohedral structure composed of alternating O-Cu-O dumbbell layers and edge-sharing $M^{III}O_6$ octahedra layers. For each Cu atom, the number of nearest-neighbor Cu atom has been halved to six. The reported optical bandgaps for delafossite $CuAlO_2$ (3.5 eV),[9,40] $CuGaO_2$ (3.6 eV),[41] and $CuInO_2$ (3.9 eV)[11] are all much wider than the bandgap of Cu_2O (2.1 eV). Using first-principles calculations, we observed that the three $CuM^{III}O_2$ compounds all exhibit indirect bandgaps with CBM located at the Γ point and VBM slightly away from the *F* point.[12] The calculated fundamental bandgap decreases from $CuAlO_2$ (at *L*) to $CuGaO_2$ (at Γ) to $CuInO_2$ (at Γ), while the experimentally measured optical bandgap increases from 3.5 eV ($CuAlO_2$) to 3.6 eV ($CuGaO_2$) to 3.9 eV ($CuInO_2$). The physical origin behind this sharp opposite trend is related to the optical transition probability. Specifically, in these delafossite compounds, the optical transition is forbidden at the Γ point due to the same parity for band edge states; the transitions probability is large near *F* and *L* points and determines the optical bandgap. The resultant large disparity between the fundamental and optical bandgap makes $CuM^{III}O_2$ as the promising bipolarly dopable TCOs, especially for $CuInO_2$.

Unlike the layered structure of $CuM^{III}O_2$, $A^{II}Cu_2O_2$ (A^{II}=Mg, Ca, Sr and Ba) crystallizes in a three dimensional (3D) tetragonal structure with a space group of $I4_1/amd$ [see Fig. 2(c)].[42] The A^{II} atom is centered on the distorted $A^{II}O_6$ octahedron with six nearest-neighbor O atoms. Though the Cu atom still forms the analogous O-Cu-O dumbbell unit as in Cu_2O, the dimension of the O-Cu-O dumbbell chain is cut down from three to one. Accordingly, in $A^{II}Cu_2O_2$ oxide, the Cu *d*-Cu *d* interaction is reduced, the VBM width

is narrowed, and the bandgap is wider compared to Cu_2O. In this sense, $A^{II}Cu_2O_2$ shares the same design concept as $CuM^{III}O_2$.

The wide bandgap for $SrCu_2O_2$ (~3.3 eV) has been experimentally confirmed, and the K-doped $SrCu_2O_2$ thin films show a p-type conductivity of 4.8×10^{-2} Scm^{-1} at room temperature.[10] Additionally, the calculated optical transition probabilities between the VBM and other bands within ~4 eV below the VBM are found to be small and negligible. The CBM of $SrCu_2O_2$ is dominated by the Cu *d* and O *p* with some Sr *s*, while the VBM has the similar orbital characters (i.e., Cu *d* and O *p* states) as that of Cu_2O. The calculated VBM hole effective masses (m_h^*) are smaller than the CBM electron effective masses (m_e^*).[13] All these results manifest that $SrCu_2O_2$ has great potential as a *p*-type TCO.

To better understand the role of A^{II} atom, we have systematically studied the electronic and optical properties of $A^{II}Cu_2O_2$ using the first-principles methods.[13] The predicted bandgaps of $MgCu_2O_2$, $CaCu_2O_2$, $SrCu_2O_2$, and $BaCu_2O_2$ are 2.45, 3.01, 3.33, and 3.01, respectively. This bandgap diversity is caused by the different atomic sizes and atomic orbital levels between different A^{II} cations, and the smaller bandgap of $BaCu_2O_2$ compared to $SrCu_2O_2$ is caused by a band crossing in the conduction bands.[13] Among these four $A^{II}Cu_2O_2$, $SrCu_2O_2$ has the widest bandgap. The alloy calculations also imply that mixing ~16% of Ca into $SrCu_2O_2$ can slightly widen the bandgap and reduce m_h^* of $SrCu_2O_2$, leading to higher conductivity and transparency.

As discussed above, the Cu^+ containing *p*-type TCOs is realized by virtue of the native *p*-type property of Cu_2O in combination with approaches to enlarge the bandgap for transparency. In view of this fact, one may ask whether it is possible to achieve *p*-TCOs based on a material that is hard to be doped *p*-type but already has a very large bandgap. Our recent work on β-Ga_2O_3 is an attempt to answer this question.[14] As an ultra-wide bandgap semiconductor with E_g = 4.8 eV, β-Ga_2O_3 has received considerable attention for its applications in ultrasensitive detectors, high power electronics, and as a deep-ultraviolet (DUV) TCO layer in diverse optoelectronic devices.[43–46] As in many other oxides, it is relatively easy to dope it *n*-type by adding Si, Ge, or Sn, yet difficult (or even impossible) to make it *p*-type.[47–50]

In order to make it *p*-type, we propose that adding a few percent of Bi into Ga_2O_3 to form dilute $(Bi_xGa_{1-x})_2O_3$ alloys could be an effective approach to raise the valence band states, so that it can be doped p-type based on the doping limit rule but leave the bandgap large enough so it is still transparent for visible light.[14] The electronic structures of Ga_2O_3 and the $(Bi_xGa_{1-x})_2O_3$ alloy are studied employing first-principles calculations. Figure 3(a) depicts a schematic of the calculated band structures for β-Ga_2O_3 and a dilute β-$(Bi_xGa_{1-x})_2O_3$ alloy. With the incorporation of Bi, an occupied intermediate valence band emerges. The intermediate valence band originates from the antibonding state of O 2p and Bi 6s, as shown in Fig. 3(b). Note that the top of the intermediate valence band is the VBM state of the β-$(Bi_xGa_{1-x})_2O_3$ alloy, which is raised by more than 1.6 eV compared to β-Ga_2O_3.

As suggested by the doping limit rule,[8] such a sufficiently high VBM energy level in alloy will greatly facilitate the *p*-type doping. However, it is observed that the commonly expected shallow acceptors Mg_{Ga} (Mg substitution on the Ga site) and Zn_{Ga} still produce deep defect levels in the $(Bi_xGa_{1-x})_2O_3$ alloy due to the polaronic character of the hole states. Whereas Cu_{Ga} can decouple the hole state and the VBM, and thereby, it is found to be a shallow acceptor in the $(Bi_xGa_{1-x})_2O_3$ alloy, despite it having a deeper defect level than that of

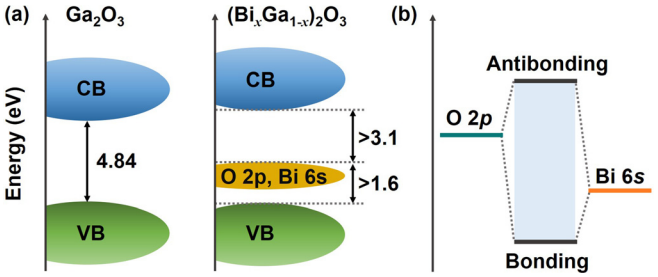

FIG. 3. (a) Schematic plot of the electronic band structures of β-Ga_2O_3 and β-$(Bi_xGa_{1-x})_2O_3$ alloy with dilute concentration. The occupied intermediate valence band dominated by the hybridized O 2*p* and Bi 6*s* orbitals is shown in yellow. (b) Schematic plot of the coupling between O 2*p* and Bi 6*s* atomic orbitals. The antibonding state is the VBM of β-$(Bi_xGa_{1-x})_2O_3$ alloy, i.e., the top of the occupied intermediate valence band.

Zn_{Ga} (Mg_{Ga}) in Ga_2O_3. These results provide insights into the doping of material systems with the strongly correlated band edge states. In addition, it is noted that the dilute $(Bi_xGa_{1-x})_2O_3$ alloy exhibits a wide bandgap $E_g > 3.1$ eV, thus the Cu-doped dilute $(Bi_xGa_{1-x})_2O_3$ alloys is expected to be a promising candidate for *p*-type TCO. In simple terms, if we refer the design avenue of Cu^+ containing TCO as a bandgap widening concept, then that of $(Bi_xGa_{1-x})_2O_3$ TCO could be designated as a bandgap narrowing concept.

The conventional TCOs generally exhibit both low-lying *s*-like CBM and *p*-like VBM, undoubtedly leading to the good *n*-type conductivity but poor *p*-type conductivity. As such, if a semiconductor displays an inverted band structure with *s*-like VBM and *p*-like CBM, in principle, the conductivity behaviors could be accordingly inverted, and the semiconductor could be a good *p*-type TCM candidate. Perovskite ABX_3 compounds containing heavy elements, such as Pb and Bi, belong to the prototype materials with the inverted band structure due to the relativistic effects.[51] Recently, we have proposed and demonstrated that the inorganic metal halide perovskites with wide bandgap could be an alternative family of *p*-type TCMs.[16]

Figure 4 depicts the crystal structure of halide perovskite $CsPbCl_3$ and its schematic band levels at the *R* point. $CsPbCl_3$ crystalizes in a simple cubic perovskite structure (space group $Pm\bar{3}m$), with Pb^{2+} cations octahedrally coordinated with anions Cl^-, and Cs^+ cations are located in the space between the corner-sharing PbO_6 octahedra.

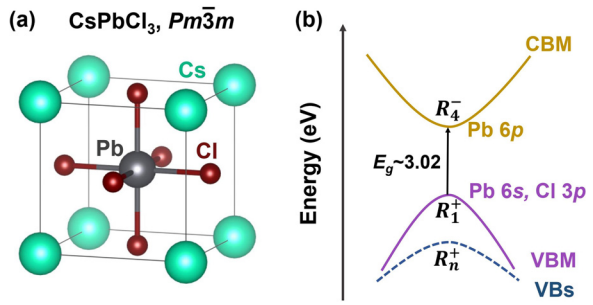

FIG. 4. (a) Crystal structure of halide perovskite $CsPbCl_3$. (b) Schematic drawing of the electronic band levels of $CsPbCl_3$ at the *R* high-symmetry point. VBs indicate the valence bands below the VBM. The irreducible representations of band states are given. For R_n^+, n = 1, 3, 4, and 5.

$CsPbCl_3$ is a direct-bandgap semiconductor with both CBM and VBM located at the R point. The R_1^+ VBM of $CsPbCl_3$ is composed of Pb 6s and Cl 3p states, while the R_4^- CBM has mostly Pb 6p character. The experimental wide bandgap of ~3.02 eV[52] ensures most of the visible-light transparency. Furthermore, it was found that the valence bands below VBM of $CsPbCl_3$ all have the even parity as VBM, indicating the forbidden electric-dipole transition between these valence bands and the resultant weak intra-band absorptions for p-type doping in $CsPbCl_3$.

Due to the inverted VBM character, the calculated hole effective mass of the VBM for $CsPbCl_3$ is only $0.21m_0$, which is comparable to the typical electron effective mass of $0.20–0.35m_0$ for n-type TCOs.[4,6,53] Additionally, the VBM is pushed up in energy by the s-p coupling, our defect calculations confirmed that it is not difficult to obtain p-type $CsPbCl_3$ under the Pb-poor condition by both intrinsic (V_{Cs}, V_{Pb}) and extrinsic (Na_{Pb}, K_{Pb}, Ag_{Pb}) defects. These results apparently imply both satisfactory conductivity and transparency for perovskite $CsPbCl_3$. The inspection of other inorganic metal halide perovskites suggests that $RbPbCl_3$ and $CsPbBr_3$ also have the potential to become high-performance p-type TCMs.

In this Perspective, we have briefly summarized the fundamental structural, electrical, and defect properties of TCMs based on our relevant first-principles studies with an emphasis on the band structure engineering and doping control of the p-type TCMs. By analyzing the unique physical properties of the prototype n-TCOs, including In_2O_3 and SnO_2, we have generalized the criteria for being a good n-type TCO: large disparity between the fundamental and optical bandgap and negligible intra-conduction band optical absorptions, which can be similarly extended to the case of p-type TCOs. On the other hand, we highlight some distinct approaches to realizing the p-type TCMs and expound the corresponding physical mechanisms (see Table I), including widening the bandgap of p-type compounds such as Cu_2O but retain its excellent electronic structure for p-type doping (such as $CuInO_2$ and $SrCu_2O_2$); raising the VBM, thus narrowing the bandgap of large bandgap compounds such as Ga_2O_3, but keeping the bandgap wide enough for transparency; and obtaining inverted band structure, i.e., the s-like VBM and p-like CBM, such as those in metal halide perovskites (e.g., $CsPbCl_3$ and $RbPbCl_3$). Similar concepts can also be applied to system like SnO and PbO.[54,55] Although these understandings above expectedly provide instructive guidelines for the scientific research and discovery of promising TCMs, there are still a variety of issues and challenges need to be addressed by future research.

While it is well known that the n-type TCOs, such as In_2O_3, SnO_2, and ZnO, can be easily doped n-type but resist p-type doping, the origin of the experimentally observed intrinsic n-type conductivity in these metal oxides remains as a controversial topic. Although many theoretical and experimental studies have demonstrated that in most of the n-type oxides, the typical intrinsic defect, oxygen vacancy (V_O), is not the origin of the n-type doping, there are still some reports suggest shallow V_O states in these TCOs. For instance, the reported (+2/0) transition energy level for ZnO lies in a wide range of 0.08–2.20 eV below the CBM.[7,56–59] There are also controversies on whether transition metal doping in these oxides is effective or not.[60]

Another issue for n-type TCMs is finding potential alternatives to ITO. Currently, ITO is the most widely used transparent conducting material in optoelectronic devices. Because indium is rare inside earth and with its increased use as TCM and in $CuInSe_2$ based solar cells,[61] it is getting more expensive, and obtaining alternative low-cost n-type TCMs with analogous or better performances than that of ITO is desirable and crucial. As a particular example, Mizoguchi *et al.* have recently found the first Ge-based ternary oxide, cubic $SrGeO_3$, as a promising n-type TCO with both good transparency and electrical conductivity.[62] The cubic perovskite $SrGeO_3$ has a fundamental bandgap of 2.7 eV and an absorption edge of 3.5 eV, fulfilling the above stated criterion of big disparity between the fundamental and optical bandgap for being a good n-type TCO. However, it is worth noting that the reported cubic $SrGeO_3$ is synthesized under 5 GPa high pressure but not at the ambient condition, which impedes its practical application as a TCO. In general, it is desirable to search high efficiency and low cost TCMs in a wider range of multicomponent composition spaces, but such an approach may also encounter difficulties because more components may also lead to more compensating defects in the doping process.

Based on the band structure engineering and doping control concept, a variety of promising alternative p-TCMs have been achieved in the past few decades, but the practical applications of p-TCMs remain immature and further efforts are needed. To realize high p-type conductivity, diverse doping avenues including multivalent element doping, complex doping, and non-equilibrium doping techniques could be pursued. Actually, the scarce knowledge about the impact of the non-equilibrium environment on the TCM performance is another vital concern in the field of TCMs. The band structure and doping properties of semiconductors are liable to be changed in the non-equilibrium environments such as low or high illumination, temperature, pressure, and electromagnetic field. Meanwhile, the exact defect type and concentration of materials under the non-equilibrium conditions are difficult to achieve because of their probable evolution over time and space. The previous doping theory is based on the equilibrium condition and is unable to be used for studying the doping behaviors in the non-equilibrium condition. Therefore, the establishment of theory

TABLE I. The key design concepts of some promising p-type TCMs.

Promising p-type TCM	Key concept
Cu^+ based ternary oxides (e.g., $CuAlO_2$, $CuInO_2$, $SrCu_2O_2$)	Widen the bandgap of p-type Cu_2O by inserting cations to reduce d-d and p-d couplings
β-$(Bi_xGa_{1-x})_2O_3$ alloy	Raise VBM and narrow the bandgap of large bandgap compound by alloying
Metal halide perovskite (e.g., $CsPbCl_3$, $RbPbCl_3$)	Employ inverted band structure with s-like VBM and p-like CBM

of non-equilibrium doping is an important opportunity and challenge in the field of TCMs and also other semiconductors.

We would like to thank P. Zhang, X. Nie, A. Walsh, S. B. Zhang, W. Ying, and H. X Deng for their helpful discussions and contributions in this work. This work was supported by the Nature Science Foundation of China (Nos. 11634003, 11991060, 12088101, and U1930402). We acknowledge the computational support from the Beijing Computational Science Research Center (CSRC).

DATA AVAILABILITY

The data that support the findings of this study are available from the corresponding author upon reasonable request.

REFERENCES

[1]K. Nomura, H. Ohta, K. Ueda, T. Kamiya, M. Hirano, and H. Hosono, "Thin-film transistor fabricated in single-crystalline transparent oxide semiconductor," Science **300**(5623), 1269 (2003).
[2]J. F. Wager, "Transparent electronics," Science **300**(5623), 1245 (2003).
[3]K. Nomura, H. Ohta, A. Takagi, T. Kamiya, M. Hirano, and H. Hosono, "Room-temperature fabrication of transparent flexible thin-film transistors using amorphous oxide semiconductors," Nature **432**(7016), 488 (2004).
[4]T. Minami, "Transparent conducting oxide semiconductors for transparent electrodes," Semicond. Sci. Technol. **20**(4), S35 (2005).
[5]C. G. Granqvist, "Transparent conductors as solar energy materials: A panoramic review," Sol. Energy Mater. Sol. Cells **91**(17), 1529 (2007).
[6]P. P. Edwards, A. Porch, M. O. Jones, D. V. Morgan, and R. M. Perks, "Basic materials physics of transparent conducting oxides," Dalton Trans. **19**, 2995 (2004).
[7]W.-J. Yin, S.-H. Wei, M. M. Al-Jassim, and Y. Yan, "Prediction of the chemical trends of oxygen vacancy levels in binary metal oxides," Appl. Phys. Lett. **99**(14), 142109 (2011).
[8]S.-H. Wei, "Overcoming the doping bottleneck in semiconductors," Comput. Mater. Sci. **30**(3-4), 337 (2004).
[9]H. Kawazoe, M. Yasukawa, H. Hyodo, M. Kurita, H. Yanagi, and H. Hosono, "P-type electrical conduction in transparent thin films of $CuAlO_2$," Nature **389**(6654), 939 (1997).
[10]H. Kawazoe, H. Yanagi, K. Ueda, and H. Hosono, "Transparent p-type conducting oxides: Design and fabrication of pn heterojunctions," MRS Bull. **25**(8), 28 (2000).
[11]H. Yanagi, T. Hase, S. Ibuki, K. Ueda, and H. Hosono, "Bipolarity in electrical conduction of transparent oxide semiconductor $CuInO_2$ with delafossite structure," Appl. Phys. Lett. **78**(11), 1583 (2001).
[12]X. Nie, S.-H. Wei, and S. Zhang, "Bipolar doping and band-gap anomalies in delafossite transparent conductive oxides," Phys. Rev. Lett. **88**(6), 066405 (2002).
[13]X. Nie, S.-H. Wei, and S. Zhang, "First-principles study of transparent p-type conductive $SrCu_2O_2$ and related compounds," Phys. Rev. B **65**(7), 075111 (2002).
[14]X. Cai, F. P. Sabino, A. Janotti, and S.-H. Wei, "Approach to achieving a p-type transparent conducting oxide: Doping of bismuth-alloyed Ga_2O_3 with a strongly correlated band edge state," Phys. Rev. B **103**(11), 115205 (2021).
[15]M. Gong, R. Sakidja, R. Goul, D. Ewing, M. Casper, A. Stramel, A. Elliot, and J. Z. Wu, "High-performance all-inorganic $CsPbCl_3$ perovskite nanocrystal photodetectors with superior stability," ACS Nano **13**(2), 1772 (2019).
[16]P. Zhang, S. Yu, X. Zhang, and S.-H. Wei, "Design of p-type transparent conductors from inverted band structure: The case of inorganic metal halide perovskites," Phys. Rev. Mater. **3**(5), 055201 (2019).
[17]A. Walsh, J. L. Da Silva, S.-H. Wei, C. Körber, A. Klein, L. Piper, A. DeMasi, K. E. Smith, G. Panaccione, and P. Torelli, "Nature of the band gap of In_2O_3 revealed by first-principles calculations and x-ray spectroscopy," Phys. Rev. Lett. **100**(16), 167402 (2008).
[18]R. Weiher and R. Ley, "Optical properties of indium oxide," J. Appl. Phys. **37**(1), 299 (1966).
[19]P. Erhart, A. Klein, R. G. Egdell, and K. Albe, "Band structure of indium oxide: Indirect versus direct band gap," Phys. Rev. B **75**(15), 153205 (2007).
[20]S. Z. Karazhanov, P. Ravindran, P. Vajeeston, A. Ulyashin, T. Finstad, and H. Fjellvåg, "Phase stability, electronic structure, and optical properties of indium oxide polytypes," Phys. Rev. B **76**(7), 075129 (2007).
[21]X. Cai, P. Zhang, and S.-H. Wei, "Revisit of the band gaps of rutile SnO_2 and TiO_2: A first-principles study," J. Semicond. **40**(9), 092101 (2019).
[22]M. Nagasawa and S. Shionoya, "Temperature dependence of the fundamental optical absorption edge in stannic oxide," J. Phys. Soc. Jpn. **30**(4), 1118 (1971).
[23]D. Fröhlich, R. Kenklies, and R. Helbig, "Band-gap assignment in SnO_2 by two-photon spectroscopy," Phys. Rev. Lett. **41**(25), 1750 (1978).
[24]K. Reimann and M. Steube, "Experimental determination of the electronic band structure of SnO_2," Solid State Commun. **105**(10), 649 (1998).
[25]A. Schleife, J. Varley, F. Fuchs, C. Rödl, F. Bechstedt, P. Rinke, A. Janotti, and C. van de Walle, "Tin dioxide from first principles: Quasiparticle electronic states and optical properties," Phys. Rev. B **83**(3), 035116 (2011).
[26]F. P. Sabino, L. N. Oliveira, S.-H. Wei, and J. L. Da Silva, "Optical and fundamental band gaps disparity in transparent conducting oxides: New findings for the and systems," J. Phys. Condens. Matter **29**(8), 085501 (2017).
[27]H. J. Snaith and C. Ducati, "SnO_2-based dye-sensitized hybrid solar cells exhibiting near unity absorbed photon-to-electron conversion efficiency," Nano Lett. **10**(4), 1259 (2010).
[28]Q. Jiang, L. Zhang, H. Wang, X. Yang, J. Meng, H. Liu, Z. Yin, J. Wu, X. Zhang, and J. You, "Enhanced electron extraction using SnO_2 for high-efficiency planar-structure $HC(NH_2)_2PbI_3$-based perovskite solar cells," Nat. Energy **2**, 16177 (2017).
[29]D. O. Scanlon, C. W. Dunnill, J. Buckeridge, S. A. Shevlin, A. J. Logsdail, S. M. Woodley, C. R. A. Catlow, M. J. Powell, R. G. Palgrave, and I. P. Parkin, "Band alignment of rutile and anatase TiO_2," Nat. Mater. **12**(9), 798 (2013).
[30]S.-H. Wei and A. Zunger, "Role of d orbitals in valence-band offsets of common-anion semiconductors," Phys. Rev. Lett. **59**(1), 144 (1987).
[31]W. A. Harrison, in *Electronic Structure of Semiconductor Heterojunctions* (Springer, 1988), p. 208.
[32]C. Park, S. Zhang, and S.-H. Wei, "Origin of p-type doping difficulty in ZnO: The impurity perspective," Phys. Rev. B **66**(7), 073202 (2002).
[33]E.-C. Lee and K.-J. Chang, "Possible p-type doping with group-I elements in ZnO," Phys. Rev. B **70**(11), 115210 (2004).
[34]J. Li, S.-H. Wei, S.-S. Li, and J.-B. Xia, "Design of shallow acceptors in ZnO: First-principles band-structure calculations," Phys. Rev. B **74**(8), 081201 (2006).
[35]A. K. Singh, A. Janotti, M. Scheffler, and C. G. van de Walle, "Sources of electrical conductivity in SnO_2," Phys. Rev. Lett. **101**(5), 055502 (2008).
[36]R. G. Gordon, "Criteria for choosing transparent conductors," MRS Bull. **25**(8), 52 (2000).
[37]B. G. Svensson, S. Pearton, and C. Jagadish, *Oxide Semiconductors* (Academic Press, 2013).
[38]J.-M. Zuo, M. Kim, M. O'keeffe, and J. Spence, "Direct observation of d-orbital holes and Cu–Cu bonding in Cu_2O," Nature **401**(6748), 49 (1999).
[39]A. Buljan, M. Llunell, E. Ruiz, and P. Alemany, "Color and conductivity in Cu_2O and $CuAlO_2$: A theoretical analysis of $d^{10}\ldots d^{10}$ interactions in solid-state compounds," Chem. Mater. **13**(2), 338 (2001).
[40]H. Yanagi, S-I. Inoue, K. Ueda, H. Kawazoe, H. Hosono, and N. Hamada, "Electronic structure and optoelectronic properties of transparent p-type conducting $CuAlO_2$," J. Appl. Phys. **88**(7), 4159 (2000).
[41]K. Ueda, T. Hase, H. Yanagi, H. Kawazoe, H. Hosono, H. Ohta, M. Orita, and M. Hirano, "Epitaxial growth of transparent p-type conducting $CuGaO_2$ thin films on sapphire (001) substrates by pulsed laser deposition," J. Appl. Phys. **89**(3), 1790 (2001).
[42]C. L. Teske and H. Muller-Buschbaum, "On our knowledge of $SrCu_2O_2$," Z. Anorg. Allg. Chem. **379**, 113 (1970).
[43]M. Higashiwaki, H. Murakami, Y. Kumagai, and A. Kuramata, "Current status of Ga_2O_3 power devices," Jpn. J. Appl. Phys. **55**(12), 1202A1 (2016).
[44]M. Baldini, Z. Galazka, and G. Wagner, "Recent progress in the growth of β-Ga_2O_3 for power electronics applications," Mater. Sci. Semicond. Process. **78**, 132 (2018).

[45]S. J. Pearton, J. Yang, P. H. Cary, F. Ren, J. Kim, M. J. Tadjer, and M. A. Mastro, "A review of Ga_2O_3 materials, processing, and devices," Appl. Phys. Rev. **5**(1), 011301 (2018).
[46]J. Y. Tsao, S. Chowdhury, M. A. Hollis, D. Jena, N. M. Johnson, K. A. Jones, R. J. Kaplar, S. Rajan, C. G. van de Walle, E. Bellotti, C. L. Chua, R. Collazo, M. E. Coltrin, J. A. Cooper, K. R. Evans, S. Graham, T. A. Grotjohn, E. R. Heller, M. Higashiwaki, M. S. Islam, P. W. Juodawlkis, M. A. Khan, A. D. Koehler, J. H. Leach, U. K. Mishra, R. J. Nemanich, R. C. N. Pilawa-Podgurski, J. B. Shealy, Z. Sitar, M. J. Tadjer, A. F. Witulski, M. Wraback, and J. A. Simmons, "Ultrawide-bandgap semiconductors: Research opportunities and challenges," Adv. Electron. Mater. **4**(1), 1600501 (2018).
[47]K. Sasaki, A. Kuramata, T. Masui, E. G. Víllora, K. Shimamura, and S. Yamakoshi, "Device-quality β-Ga_2O_3 epitaxial films fabricated by ozone molecular beam epitaxy," Appl. Phys. Express **5**(3), 035502 (2012).
[48]A. J. Green, K. D. Chabak, E. R. Heller, R. C. Fitch, M. Baldini, A. Fiedler, K. Irmscher, G. Wagner, Z. Galazka, and S. E. Tetlak, "3.8-MV/cm breakdown strength of MOVPE-grown Sn-Doped β-Ga_2O_3 MOSFETs," IEEE Electron Device Lett. **37**(7), 902 (2016).
[49]N. Moser, J. McCandless, A. Crespo, K. Leedy, A. Green, A. Neal, S. Mou, E. Ahmadi, J. Speck, and K. Chabak, "Ge-doped β-Ga_2O_3 MOSFETs," IEEE Electron Device Lett. **38**(6), 775 (2017).
[50]A. Kyrtsos, M. Matsubara, and E. Bellotti, "On the feasibility of p-type Ga_2O_3," Appl. Phys. Lett. **112**(3), 032108 (2018).
[51]W.-J. Yin, J.-H. Yang, J. Kang, Y. Yan, and S.-H. Wei, "Halide perovskite materials for solar cells: A theoretical review," J. Mater. Chem. A **3**(17), 8926 (2015).
[52]L. Protesescu, S. Yakunin, M. I. Bodnarchuk, F. Krieg, R. Caputo, C. H. Hendon, R. X. Yang, A. Walsh, and M. V. Kovalenko, "Nanocrystals of cesium lead halide perovskites ($CsPbX_3$, X= Cl, Br, and I): Novel optoelectronic materials showing bright emission with wide color gamut," Nano Lett. **15**(6), 3692 (2015).
[53]K. H. Zhang, K. Xi, M. G. Blamire, and R. G. Egdell, "P-type transparent conducting oxides," J. Phys. Condens. Matter **28**(38), 383002 (2016).
[54]A. Walsh, D. J. Payne, R. G. Egdell, and G. W. Watson, "Stereochemistry of post-transition metal oxides: Revision of the classical lone pair model," Chem. Soc. Rev. **40**(9), 4455 (2011).
[55]N. Quackenbush, J. Allen, D. Scanlon, S. Sallis, J. Hewlett, A. Nandur, B. Chen, K. Smith, C. Weiland, and D. Fischer, "Origin of the bipolar doping behavior of SnO from X-ray spectroscopy and density functional theory," Chem. Mater. **25**(15), 3114 (2013).
[56]A. Janotti and C. G. van de Walle, "Oxygen vacancies in ZnO," Appl. Phys. Lett. **87**(12), 122102 (2005).
[57]F. Oba, A. Togo, I. Tanaka, J. Paier, and G. Kresse, "Defect energetics in ZnO: A hybrid Hartree-Fock density functional study," Phys. Rev. B **77**(24), 245202 (2008).
[58]P. Ágoston, K. Albe, R. M. Nieminen, and M. J. Puska, "Intrinsic n-type behavior in transparent conducting oxides: A comparative hybrid-functional study of In_2O_3, SnO_2, and ZnO," Phys. Rev. Lett. **103**(24), 245501 (2009).
[59]J. Buckeridge, C. R. A. Catlow, M. Farrow, A. J. Logsdail, D. Scanlon, T. Keal, P. Sherwood, S. Woodley, A. Sokol, and A. Walsh, "Deep vs shallow nature of oxygen vacancies and consequent n-type carrier concentrations in transparent conducting oxides," Phys. Rev. Mater. **2**(5), 054604 (2018).
[60]J. Xu, J.-B. Liu, B.-X. Liu, S.-N. Li, S.-H. Wei, and B. Huang, "Design of n-type transparent conducting oxides: The case of transition metal doping in In_2O_3," Adv. Electron. Mater. **4**(3), 1700553 (2018).
[61]B. Huang, S. Chen, H.-X. Deng, L.-W. Wang, M. A. Contreras, R. Noufi, and S.-H. Wei, "Origin of reduced efficiency in Cu(In,Ga)Se_2 solar cells with high Ga concentration: Alloy solubility versus intrinsic defects," IEEE J. Photovolt. **4**(1), 477 (2014).
[62]H. Mizoguchi, T. Kamiya, S. Matsuishi, and H. Hosono, "A germanate transparent conductive oxide," Nat. Commun. **2**, 470 (2011).